Available online at www.sciencedirect.com
SCIENCE DIRECT®
ELSEVIER
Journal of Magnetism and Magnetic Materials 269 (2004) 327–332
journal of magnetism and magnetic materials
www.elsevier.com/locate/jmmm

Spin-filter magnetoresistance in magnetic barrier junctions

Alireza Saffarzadeh*

Department of Physics, Tehran Payame Noor University, Fallahpour Street, Nejatollahi Street, Tehran, Iran

Received 16 May 2003; received in revised form 5 July 2003

Abstract

The tunnel current and magnetoresistance (TMR) are investigated in magnetic tunnel junctions consisting of a spin-filter tunnel barrier, sandwiched between a ferromagnetic (FM) electrode and a nonmagnetic electrode. The investigations are based on the transfer matrix method and the free-electron approximation. The numerical results show that the spin transport depends on the relative magnetization orientation of the FM electrode and the spin-filter barrier, such that the tunnel current reaches its maximum when the magnetic moments of the FM electrode and the magnetic barrier are parallel. It is also found that the TMR increases with increasing the applied voltage.

PACS: 73.40.Gk; 85.75.−d; 85.70.Kh

Keywords: Magnetoresistance; Magnetic tunnel barriers; Spin filter; Spin-polarized transport

1. Introduction

Since the observation of tunnel magnetoresistance (TMR) in magnetic tunnel junctions [1], there has been a lot of interest in structures consisting of two ferromagnetic (FM) electrodes separated by one insulator or semiconductor (FM/I(S)/FM). This is due to the possible applications as magnetic field sensors and memory cells in magnetic random access memories [2,3]. The TMR in the magnetic tunnel junctions is limited by the spin polarizations of the FM electrodes. Recently, large magnetoresistance ratios as high as 30% were reported in $Fe/Al_2O_3/Fe$ [4] and $CoFe/Al_2O_3/Co$ [5].

The TMR of such FM/I(S)/FM tunnel junctions can be understood in terms of a two-band model in which the energy bands of the FM electrodes are split into spin-up and spin-down bands with different density of states at the Fermi energy. When the magnetization of the electrodes is parallel, the spin-up (spin-down) electrons tunnel from a majority (minority) spin to a majority (minority) spin band, whereas in the antiparallel alignment, the spin-up (spin-down) electrons are forced to tunnel from a majority (minority) spin to a minority (majority) spin band. This gives rise to a change in the conductance when the magnetizations are switched. During the last 10 years, a lot of theoretical papers were published on this topic (see reviews in Refs. [6,7]).

Using magnetic insulating layers, instead of having FM electrodes, one can obtain very high

*Tel.: +98-218800252; fax: +98-218808203.
E-mail address: a-saffar@tehran.pnu.ac.ir (A. Saffarzadeh).

0304-8853/$ - see front matter
doi:10.1016/S0304-8853(03)00627-9

values for the TMR [8–10]. Tunneling experiments using ferromagnetic semiconductors (FMSs), in particular the Eu chalcogenides, as the magnetic tunnel barriers [11,12], have shown spin polarization in the tunnel current which in favorable cases exceeds 99% [13]. When a magnetic barrier, which acts as spin filter, is used in a tunnel junction, due to the spin splitting of its conduction band below T_C (Curie temperature), tunneling electrons see a spin-dependent barrier height. In this case, the probability of tunneling for one spin channel will be much larger than the other, and a highly spin-polarized current may result. More recently, LeClair et al. [9] using a spin-filter barrier and an FM electrode, obtained a large TMR in an Al/EuS/Gd tunnel junction which is a new method for injecting spins into semiconductors. The spin filtering and the magnetoresistance have also been investigated theoretically in semimagnetic semiconductors [14].

In this paper, using the transfer matrix method, we study theoretically the effect of the thickness of the magnetic barrier and the applied bias on the TMR for tunneling through an FM/FMS/NM tunnel junction with an asymmetrical barrier. We assume that the electron wave vector parallel to the interfaces and the spin direction of the electron are conserved in the tunneling process through the whole system.

In Section 2, we describe the model and present a general formula for the tunneling current through the magnetic tunnel junction. Numerical results for a typical tunnel junction are presented in Section 3. A brief summary is given in Section 4.

2. Model and formalism

Consider an FM/FMS/NM sandwiched structure in the presence of DC bias V_a as shown in Fig. 1, where ϕ_L and ϕ_R are the barrier heights in the left- and right-hand side of the FMS layer above T_C, respectively. For a tunnel junction with different electrode materials, the difference in barrier height at both metal–insulator interfaces makes the barrier oblique, resulting in an asymmetric current–voltage behavior. In this case, an asymmetry parameter $\Delta\phi = \phi_L - \phi_R$ is introduced at zero bias to account for the tilted barrier potential [15]. Here we consider the case that the tunneling electron with energy E_x is incident from the left and transmits to the right along the x direction. In a free-electron approximation of the spin-polarized conduction electrons, the longitudinal part of the effective one-electron Hamiltonian may be written as

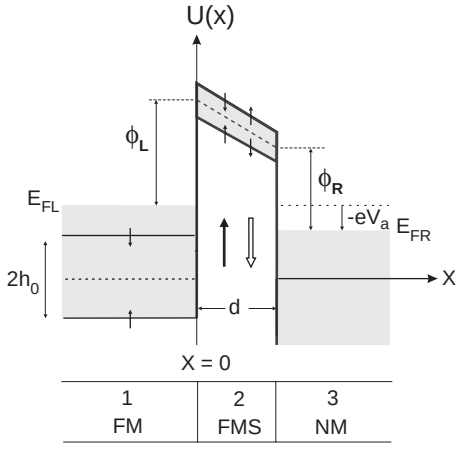

Fig. 1. Spin-dependent potential profile for FM/FMS/NM tunnel junctions in the presence of a positive bias V_a. In the FMS layer, the dashed line represents the bottom of the conduction band at $T \geqslant T_C$ and the thin arrows indicate the bottom of the conduction band for spin-up and -down electrons at $T < T_C$. The direction of magnetization in the FM layer is fixed in the $+z$, while the magnetization in the magnetic barrier is free to be flipped into either the $+z$ or $-z$ direction, as indicated by thick arrows. The zero of energy is taken at the middle of bottoms for majority-spin band and minority-spin one in the FM layer.

$$H_x = -\frac{\hbar^2}{2m_j^*}\frac{d^2}{dx^2} + U_j(x) + V^\sigma - \mathbf{h}(x)\cdot\sigma, \qquad (1)$$

where m_j^* $(j = 1\text{–}3)$ are the electron effective masses in three regions labeled in Fig. 1, and

$$U_j(x) = \begin{cases} 0, & x < 0, \\ E_{FL} + \phi_L - (\Delta\phi + eV_a)x/d, & 0 \leqslant x < d, \\ -eV_a, & x \geqslant d, \end{cases} \qquad (2)$$

where E_{FL} is the Fermi energy of the FM electrode and d is the barrier width. V^σ which is a spin-dependent potential, denotes the $s-f$ exchange

coupling between the spin of tunneling electrons and the localized f spins in the magnetic barrier. This term, within the mean field approximation, is proportional to the thermal average of the f spins, $\langle S_z \rangle$ (a $\frac{7}{2}$ Brillouin function), and can be written as $V^\sigma = -I\sigma\langle S_z\rangle$. Here, $\sigma = \pm 1$ which corresponds to $\sigma = \uparrow, \downarrow$, respectively, and I is the $s-f$ exchange constant in the FMS layer. $-\mathbf{h}(x)\cdot\sigma$ is the internal exchange energy where $\mathbf{h}(x)$ is the molecular field in the FM electrode and $|\mathbf{h}| = h_0$. Although the transverse momentum $\hbar\mathbf{k}_\parallel$ is omitted from the above notations, the summation over $\mathbf{k}_\parallel$ is carried out in our calculations.

The Schrödinger equation for a biased barrier layer can be simplified by a coordinate transformation whose solution is the linear combination of the Airy function $\mathrm{Ai}[\rho(x)]$ and its complement $\mathrm{Bi}[\rho(x)]$ [16]. Considering all three regions of the FM/FMS/NM junction shown in Fig. 1, the eigenfunctions of Hamiltonian (1) with eigenvalue E_x have the following forms:

$$\psi_{j\sigma}(x) = \begin{cases} A_{1\sigma}e^{ik_{1\sigma}x} + B_{1\sigma}e^{-ik_{1\sigma}x}, & x<0, \\ A_{2\sigma}\,\mathrm{Ai}[\rho_\sigma(x)] + B_{2\sigma}\,\mathrm{Bi}[\rho_\sigma(x)], & 0\leqslant x<d, \\ A_{3\sigma}e^{ik_3x} + B_{3\sigma}e^{-ik_3x}, & x\geqslant d, \end{cases} \tag{3}$$

where

$$k_{1\sigma} = \sqrt{2m_1^*(E_x + h_0\sigma)}/\hbar \tag{4}$$

and

$$k_3 = \sqrt{2m_3^*(E_x + eV_a + E_{FR} - E_{FL})}/\hbar \tag{5}$$

are the electron wave vectors along the x-axis. $A_{j\sigma}$ and $B_{j\sigma}$ are constants to be determined from the boundary conditions, while

$$\rho_\sigma(x) = \frac{x}{\lambda_0} + \beta_\sigma, \tag{6}$$

with

$$\lambda_0 = -\left[\frac{\hbar^2 d}{2m_2^*(\Delta\phi + eV_a)}\right]^{1/3}, \tag{7}$$

$$\beta_\sigma = \frac{[E_x - E_{FL} - \phi_L - V^\sigma]d}{(\Delta\phi + eV_a)\lambda_0}. \tag{8}$$

Upon applying the boundary conditions such that the wave functions and their first derivatives are matched at each interface point x_j, i.e., $\psi_{j,\sigma}(x_j) = \psi_{j+1,\sigma}(x_j)$ and $(m_j^*)^{-1}[\mathrm{d}\psi_{j,\sigma}(x_j)/\mathrm{d}x] = (m_{j+1}^*)^{-1}[\mathrm{d}\psi_{j+1,\sigma}(x_j)/\mathrm{d}x]$, we obtain a matrix formula that connects the coefficients $A_{1\sigma}$ and $B_{1\sigma}$ with the coefficients $A_{3\sigma}$ and $B_{3\sigma}$ as follows:

$$\begin{bmatrix} A_{1\sigma} \\ B_{1\sigma} \end{bmatrix} = M_{\mathrm{total}} \begin{bmatrix} A_{3\sigma} \\ B_{3\sigma} \end{bmatrix}, \tag{9}$$

where

$$\begin{aligned} M_{\mathrm{total}} = {} & \frac{k_3}{k_{1\sigma}} \begin{bmatrix} ik_{1\sigma} & \frac{1}{\lambda_0}\frac{m_1^*}{m_2^*} \\ ik_{1\sigma} & -\frac{1}{\lambda_0}\frac{m_1^*}{m_2^*} \end{bmatrix} \\ & \times \begin{bmatrix} \mathrm{Ai}[\rho_\sigma(x=0)] & \mathrm{Bi}[\rho_\sigma(x=0)] \\ \mathrm{Ai}'[\rho_\sigma(x=0)] & \mathrm{Bi}'[\rho_\sigma(x=0)] \end{bmatrix} \\ & \times \begin{bmatrix} \mathrm{Ai}[\rho_\sigma(x=d)] & \mathrm{Bi}[\rho_\sigma(x=d)] \\ \mathrm{Ai}'[\rho_\sigma(x=d)] & \mathrm{Bi}'[\rho_\sigma(x=d)] \end{bmatrix}^{-1} \\ & \times \begin{bmatrix} ik_3 & \frac{1}{\lambda_0}\frac{m_3^*}{m_2^*} \\ ik_3 & -\frac{1}{\lambda_0}\frac{m_3^*}{m_2^*} \end{bmatrix}^{-1} \begin{bmatrix} e^{-ik_3d} & 0 \\ 0 & e^{ik_3d} \end{bmatrix}^{-1}. \end{aligned} \tag{10}$$

Since there is no reflection in region 3, the coefficient $B_{3\sigma}$ in Eq. (3) is zero and the transmission coefficient of the spin σ electron which is defined as the ratio of the transmitted flux to the incident flux can be written as

$$T_\sigma(E_x, V_a) = \frac{k_3 m_1^*}{k_{1\sigma} m_3^*}\left|\frac{1}{M_{\mathrm{total}}^{11}}\right|^2, \tag{11}$$

where M_{total}^{11} is the left-upper element of the matrix M_{total} defined in Eq. (10).

At $T = 0\,\mathrm{K}$, the spin-dependent current density for the magnetic tunnel junction in the free-electron model is given by the formula [17]

$$\begin{aligned} J_\sigma = \frac{em_1^*}{4\pi^2\hbar^3}\Bigg[& eV_a\int_{E_0^\sigma}^{E_F - eV_a} T_\sigma(E_x, V_a)\,\mathrm{d}E_x \\ & + \int_{E_F - eV_a}^{E_F} (E_F - E_x)T_\sigma(E_x, V_a)\,\mathrm{d}E_x\Bigg], \end{aligned} \tag{12}$$

where E_0^σ is the lowest possible energy that will allow transmission and is given by $E_0^\uparrow =$

$\max\{-h_0, -(eV_a + E_{FR} - E_{FL})\}$ for spin-up and $E_0^{\downarrow} = h_0$ for spin-down electrons.

The tunnel conductance per unit area is given by $G = \sum_\sigma J_\sigma / V_a$. In this case, the TMR can be described quantitatively by the relative conductance change as

$$\mathrm{TMR} = \frac{G_{\uparrow\uparrow} - G_{\uparrow\downarrow}}{G_{\uparrow\uparrow}}, \tag{13}$$

where $G_{\uparrow\uparrow}$ and $G_{\uparrow\downarrow}$ correspond to the conductances in the parallel and antiparallel alignments of the magnetizations, respectively.

3. Numerical results

Taking the Fe/EuS/Al tunnel junction as an example, we calculate the tunnel current and TMR of the junction according to Eqs. (11)–(13). We have chosen Fe and EuS because they have cubic structures and the lattice mismatch is only 4% [18]. The appropriate parameters for EuS which have been used in this article are: $S = \frac{7}{2}, I = 0.1\,\mathrm{eV}$ [19]. The parameters E_{FL} and h_0 for Fe layer are taken corresponding to $k_{F\uparrow} = 1.09\,\text{Å}^{-1}$ and $k_{F\downarrow} = 0.42\,\text{Å}^{-1}$ (for itinerant d electrons) [20]. In the Al layer $E_{FR} = 11.7\,\mathrm{eV}$ [21]. The barrier heights at the interfaces, which can be derived from the work functions [22] of Fe and Al and the electron affinity of EuS [11], are taken as $\phi_L = 1.94\,\mathrm{eV}$ and $\phi_R = 1.7\,\mathrm{eV}$. In practice, the effective masses of electrons may differ from that of free electron, but here for simplicity, we assume all electrons have the same mass, m as free electrons. We show the numerical results at $T = 0\,\mathrm{K}$. Thus, in the case of parallel (antiparallel) alignment $\langle S_z \rangle = S$ ($\langle S_z \rangle = -S$).

In Fig. 2, the TMR is shown as a function of the width of the magnetic barrier d, when the bias voltage $V_a = 0.5\,\mathrm{V}$ is applied to the junction. At zero temperature and for the nearly normal incidence, the electrons with E_x near E_F carry most of the current. Furthermore, the Fermi energy and the barrier heights at fixed temperature, are constant. Therefore, with increasing the thickness of the EuS layer from zero, when the thickness approaches half the wavelength of the electron wave in the magnetic barrier, the tunnel conductance with the parallel alignment increases faster than with the antiparallel alignment. In this case, we can expect a peak in the TMR. By increasing the thickness further, the tunnel conductance and hence the TMR decreases exponentially.

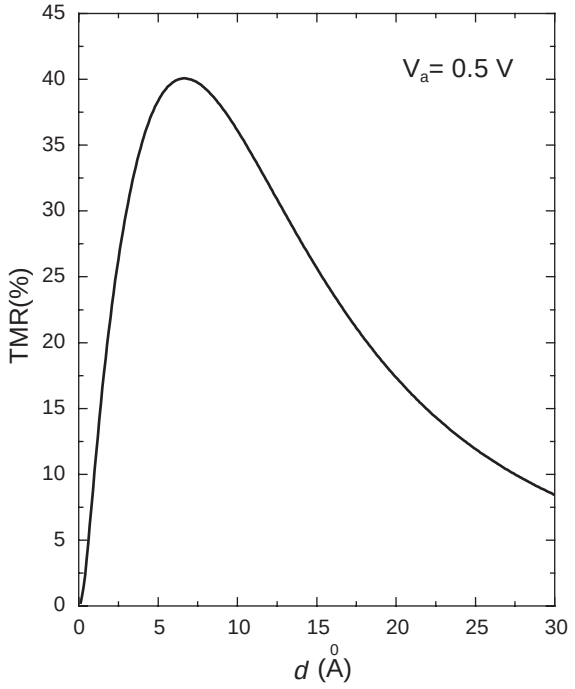

Fig. 2. Dependence of the TMR on the thickness of EuS layer.

Fig. 3 shows the spin-dependent current densities for spin-up and -down electrons as a function of applied bias. In the parallel alignment, the tunnel current for spin-up electrons is much higher than the spin-down ones, while in the antiparallel alignment, the discrepancy between the tunnel currents of the two spin channels increases very slowly. The origin of this effect is that the tunnel current for each spin channel depends on the density of states in the Fe layer and the heights of the tunnel barrier. In the parallel (antiparallel) alignment, the majority spin electrons tunnel through a barrier with low (high) height, whereas the minority spin electrons tunnel through a barrier with high (low) height, thus we can expect a high (low) spin-polarized current.

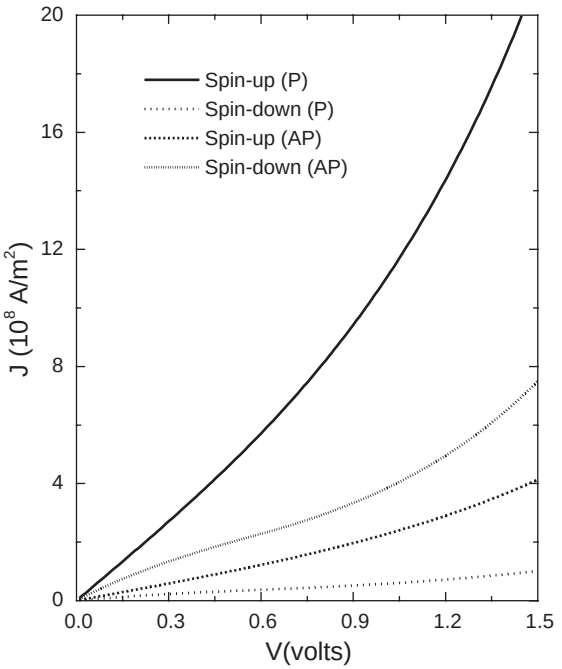

Fig. 3. Dependence of the current densities J_σ on bias voltage calculated for $d = 7$ Å in the parallel (P) and antiparallel alignments (AP).

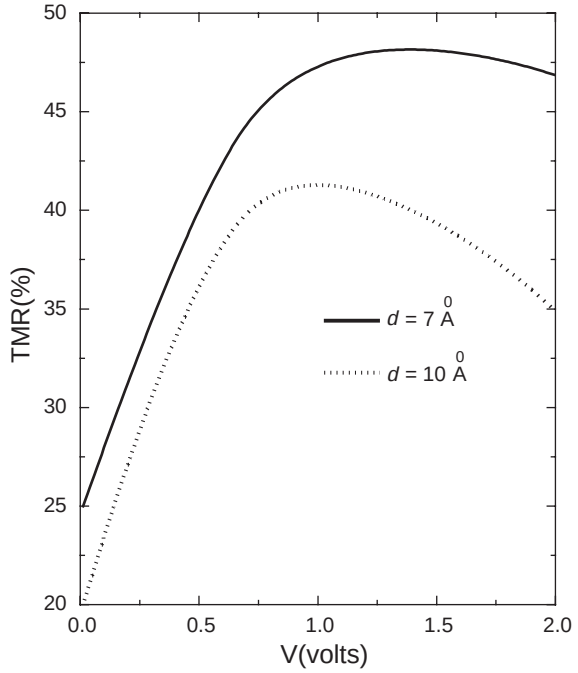

Fig. 4. Dependence of the TMR on bias voltage calculated for $d = 7$ and 10 Å.

It is clearly observed that for both the parallel and antiparallel alignments at low voltages the tunnel current curves vary linearly. With increasing the bias voltage, the effective width of the barrier becomes narrower and hence the slope of the curves increases. This effect is very strong for spin-up electrons in the parallel alignment, and causes the TMR increases with increasing the bias voltage.

In order to reveal another aspect of the spin-filtering phenomenon in the system, we have displayed the voltage dependence of the TMR in Fig. 4. As the figure shows for $d = 7$ and 10 Å, with increasing the bias voltage the TMR increases linearly and decreases at high voltages. This decrease which is not identical for different barrier thicknesses is a consequence of the narrowing of the barrier width. At low voltages, the tunneling probability for one spin channel is higher than the other, whereas at high voltages, by narrowing the barrier, this tunneling probability increases for both channels; thus, the tunnel conductance ratio, $G_{\uparrow\downarrow}/G_{\uparrow\uparrow}$, tends toward unity, and hence the TMR decreases. This dependence of the TMR on bias voltage is not similar to the results of the FM/I(S)/FM tunnel junctions [23], because in the present study, we have a spin-dependent barrier. In FM/I(S)/FM junctions, both the majority and minority electrons see identical barrier heights. In this case, as the bias voltage increases the imbalance between the number of majority and minority tunneling states diminishes and, therefore, the TMR decreases.

From these results one can see that, for the FM/FMS/NM tunnel junctions, the spin transport and hence the TMR can be controlled by the applied bias and the thickness of the FMS layer.

4. Concluding remarks

In summary, we have shown how using a magnetic barrier and an FM electrode one leads to a new magnetoresistive device. The obtained

results for spin-filter magnetoresistance show that the spin currents depends on the relative magnetization orientation of the FM electrode and the spin-filter barrier. It was also found that the low spin-polarized current will be amplified through the magnetic barrier; thus, a very large spin-polarized current from the FM electrode is injected into the NM electrode and a high value for the TMR is then obtained.

Our analysis of the TMR can be potentially useful to achieve larger TMR by optimally adjusting the material parameters. The two materials systems, ferrites and garnets [24] are both insulating and ferrimagnetic above room temperature. Therefore, they are well suited for obtaining large TMR in FM/FMS/NM. However, for successful spintronics applications, future efforts will have to concentrate on fabricating FM semiconductors in which ferromagnetism will persist at higher temperatures.

Acknowledgements

I would like to express sincere thanks to Dr. Patrick R. LeClair for helpful discussion.

References

[1] M. Julliere, Phys. Lett. A 54 (1975) 225.
[2] J.S. Moodera, L.R. Kinder, J. Nowak, P.R. LeClair, R. Meservey, Appl. Phys. Lett. 69 (1996) 708.
[3] S.S.P. Parkin, K.P. Roche, M.G. Samant, P.M. Rice, R.B. Beyers, R.E. Scheuerlein, E.J. O'Sullivan, S.L. Brown, J. Bucchigano, D.W. Abraham, Yu Lu, M. Rooks, P.L. Trouilloud, R.A. Wanner, W.J. Gallagher, J. Appl. Phys. 85 (1999) 5828.
[4] T. Miyazaki, N. Tezuka, J. Magn. Magn. Mater. 139 (1995) L231.
[5] J.S. Moodera, L.R. Kinder, T.M. Wong, R. Meservey, Phys. Rev. Lett. 74 (1995) 3273.
[6] R. Meservey, P.M. Tedrow, Phys. Rep. 238 (1994) 173.
[7] S. Zhang, P.M. Levy, Eur. Phys. J. B 10 (1999) 599.
[8] D.C. Worledge, T.H. Geballe, J. Appl. Phys. 88 (2000) 5277.
[9] P. LeClair, J.K. Ha, H.J.M. Swagten, C.H. van de Vin, J.T. Kohlhepp, W.J.M. de Jonge, Appl. Phys. Lett. 80 (2002) 625.
[10] A. Saffarzadeh, J. Phys.: Condens. Matter 15 (2003) 3041.
[11] J.S. Moodera, X. Hao, G.A. Gibson, R. Meservey, Phys. Rev. Lett. 61 (1988) 637.
[12] X. Hao, J.S. Moodera, R. Meservey, Phys. Rev. B 42 (1990) 8235.
[13] J.S. Moodera, R. Meservey, X. Hao, Phys. Rev. Lett. 70 (1993) 853.
[14] J.C. Egues, Phys. Rev. Lett. 80 (1998) 4578; J.C. Egues, C. Gould, G. Richter, L.W. Molenkamp, Phys. Rev. B 64 (2001) 195319.
[15] J.G. Simmons, Phys. Rev. Lett. 10 (1963) 10.
[16] M. Abramowitz, I.A. Stegun, Handbook of Mathematical Functions, Dover, New York, 1965.
[17] C.B. Duke, in: E. Burstein, S. Lundquist (Eds.), Tunneling Phenomena in Solids, Plenum, New York, 1969.
[18] U. Rücker, S. Demokritov, R.R. Arons, P. Grünberg, J. Magn. Magn. Mater. 269–270 (1996) 156.
[19] W. Nolting, U. Dubil, M. Matlak, J. Phys. C 18 (1985) 3687.
[20] M.B. Stearns, J. Magn. Magn. Mater. 5 (1977) 167.
[21] N.W. Ashcroft, N.D. Mermin, Solid State Physics, Holt, Rinehart and Winston, New York, 1976.
[22] S.P. Parker, Solid-State Physics Source Book, McGraw-Hill, New York, 1988.
[23] A.H. Davis, J.M. MacLaren, J. Appl. Phys. 87 (2000) 5224.
[24] R.C. O'Handley, Modern Magnetic Materials Principles and Applications, Wiley, New York, 2000.